

RESEARCH ARTICLE | JULY 05 2023

## Scaling and similarity laws in three-dimensional wall jets

Muting Hao (郝苜婷)   ; Luca di Mare 



*Physics of Fluids* 35, 075102 (2023)

<https://doi.org/10.1063/5.0140671>



[CrossMark](#)

# Scaling and similarity laws in three-dimensional wall jets

Cite as: Phys. Fluids **35**, 075102 (2023); doi: [10.1063/5.0140671](https://doi.org/10.1063/5.0140671)

Submitted: 29 December 2022 · Accepted: 7 April 2023 ·

Published Online: 5 July 2023



View Online



Export Citation



CrossMark

Muting Hao (郝苜婷),<sup>a)</sup>  and Luca di Mare 

## AFFILIATIONS

Oxford Thermo-Fluids Institute, Department of Engineering Science, University of Oxford, Oxford OX2 0ES, United Kingdom

<sup>a)</sup> Author to whom correspondence should be addressed: [muting.hao@eng.ox.ac.uk](mailto:muting.hao@eng.ox.ac.uk)

## ABSTRACT

Wall jets appear in many situations of technological and scientific interest. In gas turbines, flows produced by the film as well as impingement cooling devices are three-dimensional wall jets. High-lift devices produce flows that can easily be represented by two-dimensional wall jets. It has been known for a long time that wall jets in both stagnant and moving environments display a layered structure and only partially obey similarity laws. In this paper, we derive scaling laws and obtain self-similar velocity defect and Reynolds stress profiles for the outer part of three-dimensional wall jets in the high-Reynolds-number limit. The scaling laws are derived from prime principles under realistic assumptions about the behavior of the flow. We show that the leading term in an expansion of the turbulent kinetic energy (TKE) as a series of powers of the distance from the source must scale like the transversal velocity causing the jet to spread laterally. Only the second term in the TKE expansion is shown to scale like the square of the velocity defect. The scaling laws are tested on numerical and experimental data representing two commonly used film cooling devices.

© 2023 Author(s). All article content, except where otherwise noted, is licensed under a Creative Commons Attribution (CC BY) license (<http://creativecommons.org/licenses/by/4.0/>). <https://doi.org/10.1063/5.0140671>

## I. INTRODUCTION

Film cooling is a well-established technology to manage the temperature of solid components exposed to very hot streams. Film cooling is indispensable in modern gas turbine engines as it allows the operation of high-pressure turbine blades at gas temperatures far exceeding the melting temperature of the metal. Despite its numerous applications, few theoretical studies exist of the flow field of a film cooling device from a purely fluid mechanic point of view. The closest canonical flow to the flow produced by a film cooling device is a wall jet (Fig. 1). A wall jet is a flow produced by a slot or an orifice placed near a solid wall and ejecting fluid to flow near the wall in the direction parallel to the wall or by a jet impinging orthogonally on a wall. Wall jets and film cooling flows display features common to both jets and boundary layers.

The velocity profiles of wall jets are usually parameterized with respect to the maximum velocity  $U_m$  and its distance from the wall  $y_m$ , see Fig. 2(a). Especially in experimental studies, it is easier to identify the distance from the wall where the velocity is  $U_m/2$ . This distance is customarily denoted as  $y_{m/2}$  and is commonly used as a length scale for the study of wall jets. In wall-wakes and wall jets produced by film cooling devices, no local maximum of velocity can be identified. The velocity defect  $\Delta U$  with respect to the free-stream velocity  $U_e$  is also

monotonic. In this case, it is convenient to base the definition of the wall jet length scale on the distance  $\delta_{99}$  where the mean velocity profile attains 99% of its free stream value  $U_e$ . In this case, the velocity defect  $\Delta U_m$  evaluated at  $y/\delta_{99} = 1/2$  is a suitable scale for the velocity profile. Diagrams showing the relation between the velocity profile and the quantities  $\Delta U_m$  and  $\delta_{99}$  are shown in Figs. 2(b) and 2(c). For some film cooling jets, such as those produced by cylindrical films, the jet is lifted off the wall and a maximum velocity defect  $\Delta U_m$  can be identified, see Figs. 2(d) and 2(e).

Early interest in film cooling and wall jets arose because of cooling needs in rocket engine combustion chambers.<sup>4</sup> The first set of published wall jet measurements was performed by Förthmann,<sup>5</sup> who referred to it as a “partially open jet.” Because of its implications on correlations for friction and heat transfer in cooling flows, the scaling of velocity and Reynolds stress profiles in wall jets is a matter of considerable interest and is the subject of a considerable body of the literature dating back to the years before World War II.

Over time, contrasting results have been proposed by a host of researchers. The current understanding is that the inner (near the wall) and outer (away from the wall) regions of a wall jet follow different scaling laws, but no broad consensus exists on the scaling of the Reynolds stress profiles or the terms in their budgets.

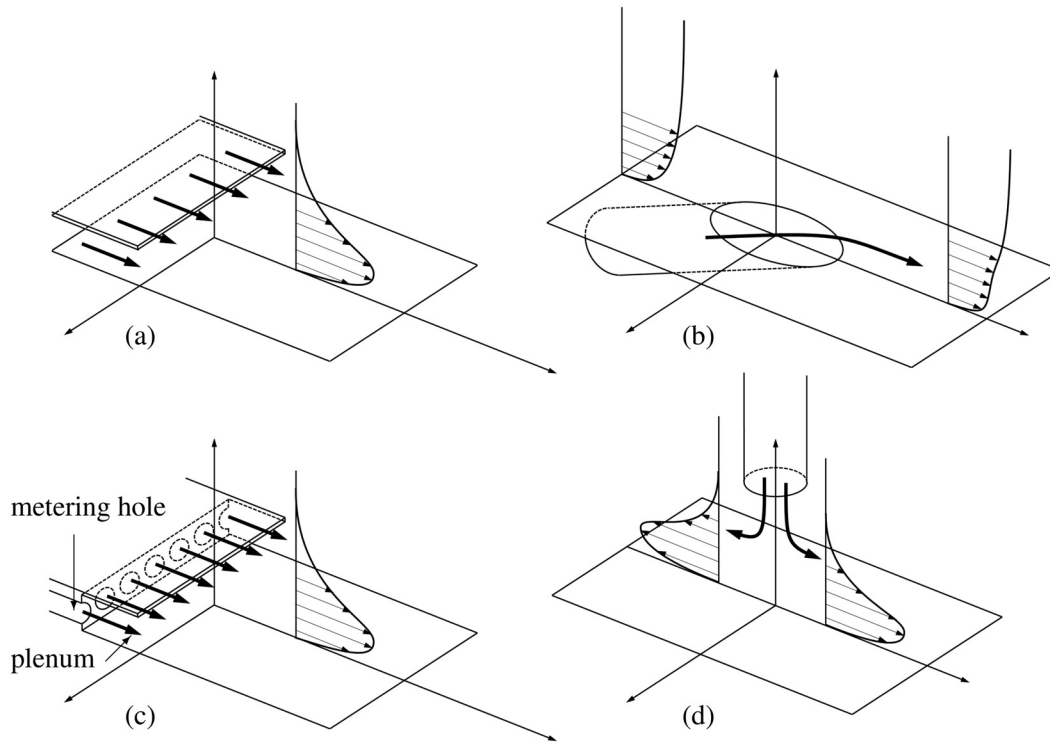


FIG. 1. Flow arrangements for typical wall jets. (a) Two-dimensional wall jet,<sup>1</sup> (b) cooling film,<sup>2</sup> (c) cooling slot,<sup>3</sup> and (d) impinging wall jet.<sup>1</sup>

The following review summarizes some important results with a view to identify aspects of previous theoretical and experimental studies that can be used with advantage in a derivation of scaling laws for wall jets from prime principles.

### A. Known results on wall jet scaling

Förthmann<sup>5</sup> determined that the velocity profile in his measurements collapsed onto a single curve with the transformation

$$\frac{U}{U_m^p} = f\left(\frac{y}{y_{m/2}}\right). \quad (1)$$

Förthmann also suggested that  $p = 1/2$  and  $y_{m/2} \approx (x_0 + x)^q$ , with  $q \approx 1$ , based on data on the outer edge of the jet. Förthmann was aware of theoretical grounds that a different scaling may be necessary near the wall and, based on a  $1/7$ -power law velocity profile, suggested that near the wall,

$$\frac{U}{U_m^p} = f\left(\frac{y}{x^q}\right) \quad (2)$$

with  $q \approx 0.9$ . Förthmann also erroneously identified the location of maximum velocity as the location of zero turbulent shear stress. Liepmann and Laufer<sup>6</sup> showed that the  $1/7$  power law is not adequate to describe the velocity profile near the wall and called into question the hypothesis of a constant mixing length for the wall jet.

The wall jet problem was reexamined in the 1950s as the range of possible applications grew from rocket engines to the combustor and

turbine cooling, high-lift devices, and deicing, to name a few. Glauert<sup>7</sup> proved that a laminar wall jet admits self-similar solutions, but a turbulent wall jet does not obey complete similarity because of the different scaling of the eddy viscosity in the inner and outer parts of the jet. Glauert obtained a self-similar solution by postulating an eddy viscosity consistent with the  $1/7$  power law near the wall and a constant eddy viscosity in the outer part of the flow. The two profiles were matched at the location of the maximum velocity, where the stress was assumed to be zero. Glauert's results for a planar wall jet call for a velocity profile with

$$U_m \approx x^{-1.15}, \quad (3)$$

$$y_{m/2} \approx x^{1.015}. \quad (4)$$

Glauert's results were partly based on measurements taken by Bakke<sup>8</sup> in a radial wall jet. The numerical constants in the power laws observed by Bakke differed slightly from those predicted by Glauert. Glauert's analysis was also corroborated by Sigalla's data.<sup>9,10</sup> Schwarz and Cosart<sup>11</sup> obtained hot wire measurements of the mean velocity profile in wall jets but not of the Reynolds stresses. They also concluded that the outer part of the velocity profile is self-similar and that the similarity variables are  $U_m$  and the jet layer thickness  $\delta$ . Their analysis showed that  $U_m$  must scale with the distance with a power no greater than  $-1/2$  and that  $\delta$  must be linear with respect to distance. Schwarz and Cosart adopted the assumption that the wall layer and the external layer are weakly coupled in their derivation of the similarity parameters and analyzed the wall layer and friction law separately.

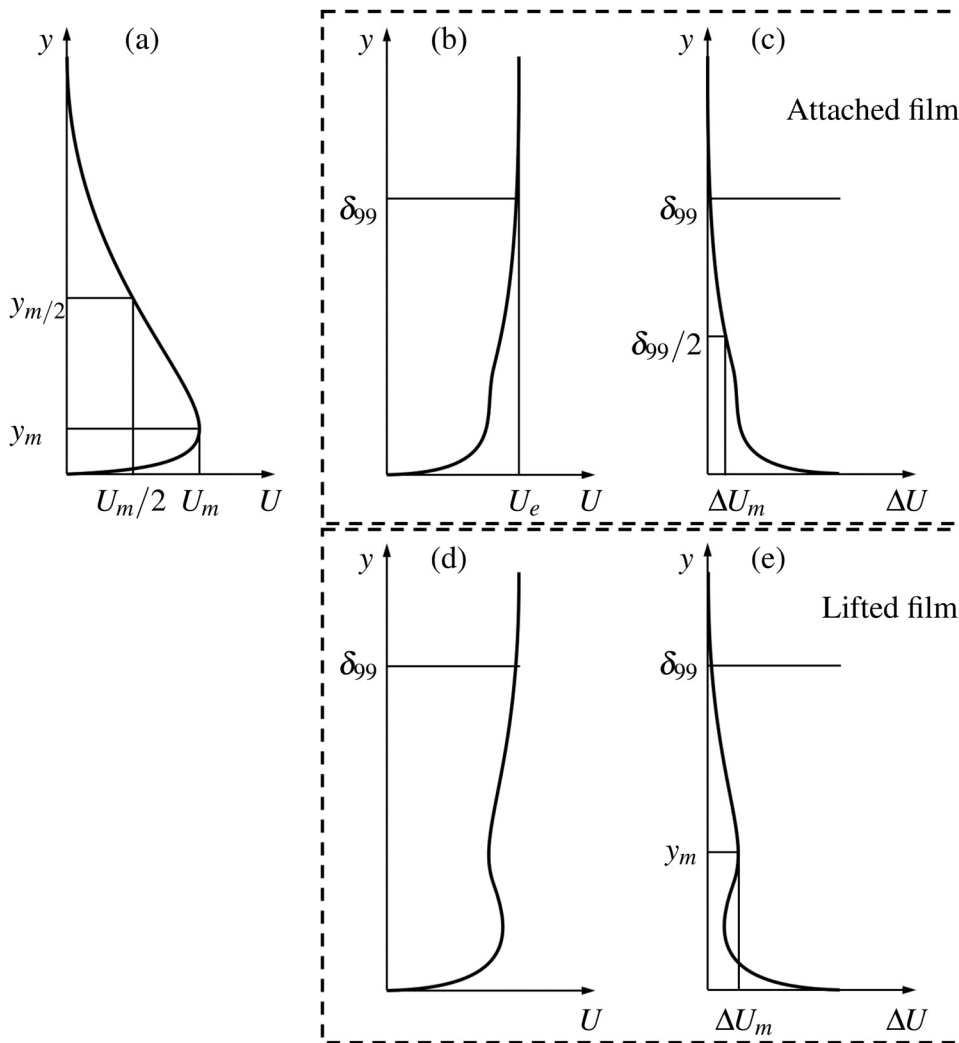


**FIG. 2.** Wall jet and film cooling jet nomenclature. (a): wall jet; (b) attached cooling film jet velocity profile; (c) attached cooling film jet velocity defect profile; (d) lifted cooling film jet velocity profile; and (e) lifted cooling film jet velocity defect profile.

Verhoff<sup>12</sup> conducted his analysis based on the assumption that the similarity could be enforced simultaneously in the inner layer and in the outer layer of the wall jet at least over a moderate range of Reynolds numbers. Verhoff also introduced a  $1/7$  power law profile as a computational device to derive a universal velocity profile. A similar expression was found in the case of a finite free-stream velocity, but with corrections in the shape of a polynomial expression in the parameter  $\zeta = U_\infty/V_j$ . Verhoff avoided difficulties with Glauert's assumptions about the eddy viscosity by solving directly for a shear stress profile, which could be expressed in terms of the function  $f$  and its integrals. Furthermore, Verhoff showed that there must be a relation between the maximum velocity and the local thickness  $\delta$  of the jet layer for a given velocity ratio  $M$  and that this relation must be of the type

$$U_m \approx (1 + M)\delta^{-\lambda}, \quad (5)$$

for a suitable constant  $\lambda$ . Similarly, the wall stress must obey a relation of the type

$$u_\tau^2 = -\alpha(1 + M)^2 \frac{d}{dx} \delta^{1-\frac{1}{\lambda}}. \quad (6)$$

By comparing the kinetic energy of the wall jet with that of a free jet, Verhoff finally showed that the jet thickness must vary exponentially with distance from the orifice,

$$\delta = ce^{d(\frac{1}{\lambda}-1)}, \quad (7)$$

for a suitable choice of the constants  $C$  and  $D$ . Kruka and Eskinazi<sup>13</sup> performed measurements and analysis of wall jets in moving streams and found that the maximum velocity  $U_m$ , its location  $y_m$ , and the maximum Reynolds shear stress  $\tau_m$  are sufficient to collapse mean velocities, turbulence intensities, and Reynolds stress onto universal profiles. They also found that

$$U_m \approx x^{-\alpha}, \quad (8)$$

$$u_\tau \approx x^{-2\alpha}. \quad (9)$$

Poreh *et al.*<sup>14</sup> studied the axisymmetric wall jet created by a round jet impinging on a wall and attempted to determine universal velocity and turbulent stress profiles based on the local maximum velocity profile and jet thickness. These in turn were found to scale with

$$U_m b / \sqrt{K} = F_m (\sqrt{K} / \nu) (r/b)^m, \quad (10)$$

$$\delta/b = F_n (\sqrt{K} \nu) (r/b)^{n-1}, \quad (11)$$

$$\tau b^2 / \rho K = F_\tau (\sqrt{K} \nu) (r/b)^{2m+n-1}, \quad (12)$$

where  $b$  is the distance from the geometrical origin of the similarity of the circular jet to the boundary, and  $K$  is the kinematic momentum flux of the circular jet leaving the orifice. They noticed that friction data do not corroborate Glauert's assumption that Blasius' friction law holds, nor that the Reynolds stress follows an eddy-viscosity type behavior. Furthermore, Poreh *et al.* found that the turbulence intensities in a wall jet are higher than those in the corresponding pipe flow and that the high turbulence intensities are responsible for a modification in the slope and intercept of the velocity profile in the logarithmic region. Poreh's data did not show collapse of the turbulence quantities with the proposed scaling parameters. Scatter in the hot wire data were offered as a possible explanation.

Bradshaw and Gee<sup>15</sup> studied wall jets within the context of boundary layer control and took hot wire measurements of jets flowing along flat and curved walls. They were the first to point out a major flaw in Glauert's solution, namely, the non-vanishing shear stress at the location of maximum velocity. They consequently took a stern view on the possibility of formulating numerical predictions for wall jets.

Kacker and Whitelaw<sup>16,17</sup> produced a detailed survey of wall jets and wall wakes based on hot-wire anemometry and published data on mean velocity profiles, turbulence intensities, Reynolds shear stress, spectra, correlation coefficients, and even selected terms in the turbulent kinetic energy (TKE) budgets, but did not attempt any form of normalization and did not discuss self-similarity properties exhibited by their results.

Significant contributions to the understanding of the evolution of wall jets at moderate distances from their injection slot were made by Sturgess.<sup>3</sup> Sturgess studied the wall jet produced by cooling slots in combustion chambers with a view to correlating effectiveness<sup>18</sup> data. Sturgess started from the observations that (i) most experimental studies are conducted on geometries not closely related to those found in actual combustors and (ii) data from different campaigns cannot be collapsed using commonly applied correlations. Sturgess attributed discrepancies to the existence of a potential core in the wall jet, which effectively offsets the start of the self-similar region from the geometric point of injection and produced a model to predict the potential core length. Sturgess<sup>19–21</sup> later revisited the issue of turbulence generation in cooling slots and correlated the performance of the slot with the extent to which turbulence and flow non-uniformity contribute to mixing in the early history of the jet itself. Turbulence and flow non-uniformity, in turn, was determined by the conditions in the plenum downstream of the metering holes.

Hammond<sup>22</sup> produced a unified velocity profile for the inner and outer region of the wall jet in stagnant surroundings by merging Spalding's universal velocity profile<sup>23</sup> and Coles<sup>24</sup> law of the wake. Hammond also derived a series of ancillary relations illustrating power laws between the main parameters of the flow, e.g.,  $U_m$ ,  $y_m$ , the

downstream distance from the slot, and the local friction velocity. Hammond showed that the velocity profiles for a wall jet in inner coordinates do not comply to the same universal logarithmic law of the wall as equilibrium boundary layers.

Lauder and Rodi<sup>25</sup> conducted a thorough review of the literature on measurements and modeling of wall jets up to 1983. Launder and Rodi summarized the state of understanding of turbulent wall jets up to that year by postulating scaling of the velocity profile with  $U_m$  and linear growth of  $y_{m/2}$  with distance from the source of the jet.

Wyganski *et al.*<sup>26</sup> studied mean velocity profile and Reynolds shear stress in planar wall jets. Wyganski *et al.* found that the maximum velocity  $U_m$  and its position  $y_{m/2}$  make the outer part of the velocity profiles collected at different distances from the origin of the jet collapse onto a single line. They introduced the jet momentum flux into their scaling laws and showed from their results that

$$U_m \approx (x - x_0)^{-0.47}, \quad (13)$$

$$y_{m/2} \approx x^{0.88}, \quad (14)$$

$$\tau_w \approx x^{-1.07}. \quad (15)$$

Wyganski *et al.* also concluded against the possibility of matching velocity profiles to the logarithmic law of the wall. Remarkably, Wyganski *et al.* found it impossible to obtain collapse of their turbulence intensities.

Zhou and Wyganski<sup>27</sup> focused their analysis on the outer part of velocity profiles of wall jets with a finite free-stream velocity and showed that as long as the ratio of jet velocity to free-stream velocity  $U_m/U_e$  is greater than 2, all available data can be made to collapse onto a universal profile of the type

$$\frac{U - U_e}{U_m - U_e} = f\left(\frac{y - y_m}{y_{m/2} - y_m}\right). \quad (16)$$

They also showed that essentially all the macroscopic parameters of the flow could be collapsed onto universal power laws if the momentum thickness was introduced in the analysis.

Eriksson *et al.*<sup>28</sup> reported detailed measurements of mean and turbulent flow quantities and scaling parameters and reported confirmation of the mutual scaling of the maximum velocity and the jet layer thickness, with an exponent close to  $-1$ :  $\log(U_m) \approx -1.083 - 0.573 \log(y_{1/2})$ . They also found a linear growth rate  $y_{1/2}/b = 0.0782(x/b) + 0.332$ . Eriksson *et al.* also reported normal and shear Reynolds stresses normalized against the local maximum velocity in the wall jet, showing that full similarity is not attained for the Reynolds stresses in external coordinates.

George *et al.*<sup>29</sup> proposed a set of scaling laws based on the friction velocity  $u^*$  for the wall layer and the maximum velocity  $U_m$  for the outer layer based on the results by Eriksson *et al.* as well as other sources. They showed that the inner and outer layers are not as weakly coupled as initially postulated by Glauert<sup>7</sup> and on the contrary a residual dependence on the length scale ratio  $u^* y_{1/2} / \nu$ . One of the interesting results obtained by George *et al.* is that the wall-normal Reynolds stress and the Reynolds shear stress scale with different quantities, namely,  $U_m$  and  $u^*$ . They also found that the maximum velocity must scale with an exponent no larger than  $-1/2$  with respect to downstream distance.

Barenblatt *et al.*<sup>30</sup> revisited the planar wall jet and showed two separate scaling laws in action for the inner and outer layer,

$$y/\gamma_m^t \approx x^{0.93}, \quad (17)$$

$$y/\gamma_m^w \approx x^{0.68}. \quad (18)$$

A recent contribution to the literature on wall jets was made by Gupta *et al.*,<sup>31</sup> who derived a universal velocity profile for the buffer layer between the wall and the maximum velocity and showed that the correct coordinate for this part of the flow is rescaled by  $\sqrt{Re_\tau}$ .

Studies on three-dimensional jets started appearing in the literature later than studies on two-dimensional jets. Sforza and Herbst<sup>32</sup> studied three-dimensional wall jets from rectangular orifices. They identified the effect of the jet potential core on the decay rate of the jet and showed the existence of two separate ranges for the spread of a three-dimensional wall jet and determined power laws describing the lateral and vertical growth of the jet, as well as the decay of the maximum velocity. The findings of Sforza and Herbst were reproduced by Kirkpatrick and Kenyon<sup>33</sup> a few years later but in the context of wall jets for air conditioning. Newman *et al.*<sup>34</sup> studied the three-dimensional wall jet issuing from a round hole. They found that the jet has a considerable lateral spread: The jet spreads laterally about seven times faster than it spreads in the direction normal to the wall. The mean velocity components attain self-preserving profiles, but the turbulence intensities do not, even if normalized by a local velocity scale. Swamy and Bandyopadhyay<sup>35</sup> conducted similar investigations. Swamy and Bandyopadhyay were able to identify not only the power-law spread regime and the radial-like spread regime but also the potential core of their jets. They found that the span-wise and wall-normal spread of the jet requires two separate virtual origins. They found no collapse of the turbulent quantities. A recent campaign of measurements in a three-dimensional wall jet was conducted by Namgyal and Hall,<sup>36</sup> who reported detailed measurements of mean velocity and six Reynolds stresses. Namgyal and Hall also reported estimates of individual TKE production terms and of the overall arrangement of the flow.

In their 1983 review, Launder and Rodi<sup>25</sup> examined the physical mechanism for the fast lateral spread of three-dimensional wall jets and tentatively identified streamline turning and Reynolds stress anisotropy as possible reasons. In a later contribution, Craft and Launder<sup>37</sup> examined the question of the lateral spread more in detail by attempting the computation of self-similar two-dimensional solutions based on Reynolds-stress transport models. They concluded that the axial vorticity and the lateral spread of the jet are driven by Reynolds stress anisotropy, very much like the secondary flow in a square duct. Craft and Launder produced flow visualizations closely resembling those produced by Sturgess<sup>19</sup> in his study of turbulence at the exit of combustor cooling slots.

It is clear from this brief review that whereas some consensus exists on the scaling of mean velocity profiles in two- and three-dimensional wall jets, no such agreement exists on the scaling of turbulent quantities with local parameters and with the downstream distance. This paper derives such novel scaling laws from first-principles, invoking the conservation of mass, momentum, and energy fluxes for the outer part of the wall jet, neglecting the loss of momentum to the wall as a first approximation. The overall conservation equations are stated in Sec. II A. A small perturbation theory valid at large distances from the orifice is developed in Sec. II B, and estimates of growth rate, entrainment, and transversal velocity scales are derived in Sec. II C. The theory is corroborated by large eddy simulation (LES) data in Sec. III.

## II. THEORY

Consider the flow generated by a wall jet, such as a film cooling device. The wall jet is idealized as a rectangular region as shown in Fig. 3 where the fluid emitted by the film (the coolant) is partially mixed with the hot stream. The jet is surrounded by unperturbed coolant. The flow is developing along a wall and is subject to no imposed pressure gradients. The flow takes place predominantly in the stream-wise direction in the hot stream. In the wall jet, the flow has components orthogonal to the free stream and these are assumed to be comparable in magnitude to the turbulent intensity.

### A. Overall conservation equations

The mass, momentum, and total enthalpy fluxes crossing surfaces located at constant streamwise positions are

$$\mathcal{F} = \iint \rho U dy dz, \quad (19)$$

$$\mathcal{G} = \iint \rho U^2 dy dz, \quad (20)$$

$$\mathcal{H} = \iint \rho U h^0 dy dz. \quad (21)$$

The integrals in Eqs. (19)–(21) can be written as sum of contributions from the wall jet and the free stream,

$$\mathcal{F} = \iint_S (\rho_c U_c - \rho_e U_e) dy dz + \iint \rho_e U_e dy dz, \quad (22)$$

$$\mathcal{G} = \iint_S (\rho_c U_c^2 - \rho_e U_e^2) dy dz + \iint \rho_e U_e^2 dy dz, \quad (23)$$

$$\mathcal{H} = \iint_S (\rho_c U_c h_c^0 - \rho_e U_e h_e^0) dy dz + \iint \rho_e U_e h_e^0 dy dz. \quad (24)$$

The wall jet is idealized as a region of approximately uniform flow properties. This is a theoretical device often used in fluid mechanics and applied to problems ranging from droplet impact to studies on geophysical jets. The quantities estimated in our analysis determine the scaling of the velocity and temperature profiles rather than their precise shape. Since the flow properties are uniform within the wall jet and the free stream, the integrals are straightforward products,

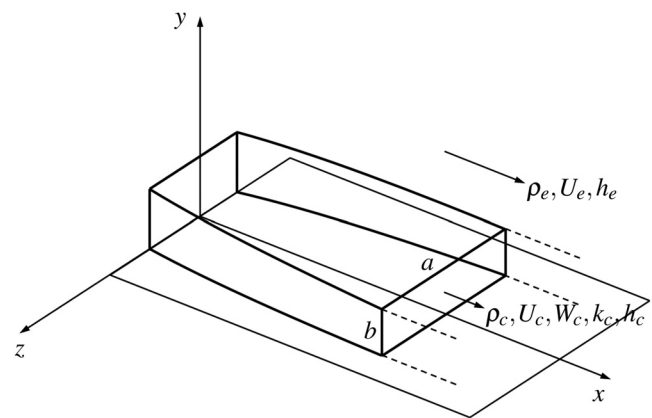


FIG. 3. Downstream development of a film cooling jet.



$$\mathcal{F} = S(\rho_c U_c - \rho_e U_e) + A \rho_e U_e, \quad (25)$$

$$\mathcal{G} = S(\rho_c U_c^2 - \rho_e U_e^2) + A \rho_e U_e^2, \quad (26)$$

$$\mathcal{H} = S(\rho_c U_c h_c^0 - \rho_e U_e h_e^0) + A \rho_e U_e h_e^0, \quad (27)$$

where the limit  $A \rightarrow \infty$  is intended, and  $S = a \cdot b$  is the cross-sectional area of the wall jet.

Before processing, it is useful to write the total enthalpy in terms of kinetic and static enthalpy contributions,

$$h_c^0 = \frac{\gamma}{\gamma - 1} \frac{P}{\rho_c} + \frac{1}{2} (U_c^2 + W_c^2) + k_c, \quad (28)$$

$$h_e^0 = \frac{\gamma}{\gamma - 1} \frac{P}{\rho_e} + \frac{1}{2} U_e^2. \quad (29)$$

The contribution of the wall-normal component to the kinetic energy of the fluid within the jet is for now neglected: The validity of this approximation will be discussed more in detail in the limit of large distance from the origin. Conservation laws for mass, momentum, and energy can now be written comparing the fluxes at two nearby stream-wise stations to find

$$\frac{d\mathcal{F}}{dx} = 0, \quad (30)$$

$$\frac{d\mathcal{G}}{dx} = 0, \quad (31)$$

$$\frac{d\mathcal{H}}{dx} = 0. \quad (32)$$

Friction at the wall is neglected in Eq. (31). Friction at the wall can be ignored based on the analysis of Schwarz and Cosart<sup>11</sup> and later Gupta *et al.*<sup>31</sup> who showed that the outer layer of the wall jet is only weakly coupled with the wall layer. Within the present analysis, it is shown that the wall stress must be a second-order perturbation on the momentum equation with respect to the leading terms. Substituting the expressions for the fluxes (25)–(27) in Eqs. (30)–(32) and keeping into account that the free stream quantities are constant, one finds

$$\frac{d}{dx} S \rho_c U_c - \rho_e U_e \frac{dS}{dx} = 0, \quad (33)$$

$$\frac{d}{dx} S \rho_c U_c^2 - \rho_e U_e^2 \frac{dS}{dx} = 0, \quad (34)$$

$$\frac{d}{dx} S \rho_c U_c h_c^0 - \rho_e U_e h_e^0 \frac{dS}{dx} = 0. \quad (35)$$

The equations can be further manipulated by substituting the continuity equation [Eq. (33)] into the momentum and energy equations [Eqs. (34) and (35)],

$$\frac{d}{dx} \rho_c U_c + (\rho_c U_c - \rho_e U_e) \frac{1}{S} \frac{dS}{dx} = 0, \quad (36)$$

$$\rho_c U_c \frac{dU_c}{dx} + \rho_e U_e (U_c - U_e) \frac{1}{S} \frac{dS}{dx} = 0, \quad (37)$$

$$\rho_c U_c \frac{dh_c^0}{dx} + \rho_e U_e (h_c^0 - h_e^0) \frac{1}{S} \frac{dS}{dx} = 0. \quad (38)$$

We now introduce the following non-dimensional variables:

$$\rho = \rho_c / \rho_e,$$

$$U = U_c / U_e,$$

$$W = W_c / U_e,$$

$$\kappa = k_c / U_e^2,$$

$$\xi = x / D,$$

$$\zeta = z / D,$$

$$\sigma = S / D^2.$$

Total enthalpies can be non-dimensionalized, thus

$$\frac{h_e^0}{U_e^2} = \frac{1}{(\gamma - 1) M_e^2} + \frac{1}{2}, \quad (39)$$

$$\frac{h_c^0}{U_e^2} = \frac{1}{\rho(\gamma - 1) M_e^2} + \frac{1}{2} (U^2 + W^2) + \kappa. \quad (40)$$

Let

$$\mathcal{M}^2 = (\gamma - 1) M_e^2. \quad (41)$$

The non-dimensional form of the conservation equations becomes

$$\frac{d}{d\xi} \rho U + (\rho U - 1) \frac{1}{S} \frac{dS}{d\xi} = 0, \quad (42)$$

$$\rho U \frac{dU}{d\xi} + (U - 1) \frac{1}{S} \frac{dS}{d\xi} = 0, \quad (43)$$

$$\rho U \frac{d}{d\xi} \left( \frac{1}{\rho \mathcal{M}^2} + \frac{1}{2} (U^2 + W^2) + \kappa \right) + \left( \frac{1}{\mathcal{M}^2} \left( \frac{1}{\rho} - 1 \right) + \frac{1}{2} (U^2 + W^2 - 1) + \kappa \right) \frac{1}{S} \frac{dS}{d\xi} = 0. \quad (44)$$

## B. Small perturbation theory

We now focus on the evolution of the wall jet far downstream of its source. As the jet travels downstream, it mixes with its surroundings so that the velocity and temperature of the jet approached the free-stream values. As the jet travels downstream, its effect on the flow becomes weaker and weaker and the non-dimensional quantities describing its behavior can be represented in terms of negative powers of the distance  $\xi$  in the following equations:

$$\rho \approx \rho_1 \xi^{-\alpha}, \quad (45)$$

$$U \approx U_1 \xi^{-\alpha} + 1, \quad (46)$$

$$W \approx W_1 \xi^{-\beta}, \quad (47)$$

$$\kappa \approx \kappa_1 \xi^{-\chi}, \quad (48)$$

$$\sigma \approx \sigma_1 \xi^{\theta}. \quad (49)$$

The velocity defect  $\Delta U$  is  $\Delta U = -U_e U_1 \xi^{-\alpha}$ . At a large distance from the film,  $\xi \gg 1$ , and for positive  $\alpha, \beta, \chi$ , the powers of  $\xi$  appearing in Eqs. (45)–(48) are small. This observation will be exploited when obtaining approximate relations from the conservation laws in the limit  $\xi \gg 1$ . From the ansatz 45–49, the following useful expressions are obtained:

$$\frac{1}{S} \frac{dS}{d\xi} = \frac{\theta}{\xi}, \quad (50)$$

$$\rho U = 1 + \xi^{-\alpha}(\rho_1 + U_1) + \xi^{-2\alpha}\rho_1 U_1. \quad (51)$$

Substituting Eqs. (50) and (51) in the continuity equation Eq. (42) yields

$$(\theta - \alpha)\xi^{-\alpha-1}(\rho_1 + U_1) + \mathcal{O}(\xi^{-2\alpha-1}) = 0. \quad (52)$$

Retaining only terms of order  $\mathcal{O}(\xi^{-\alpha-1})$  and neglecting terms of order  $\mathcal{O}(\xi^{-2\alpha-1})$  yields

$$\theta = \alpha. \quad (53)$$

The momentum equation is also identically satisfied by the condition in Eq. (53), with an error of order  $\mathcal{O}(\xi^{-2\alpha-1})$ . If wall friction terms are included in the momentum balance for the wall jet, they must also be  $\mathcal{O}(\xi^{-2\alpha-1})$ . In the energy equation, collecting equal powers of  $\xi$ , we find that the terms containing  $\rho'$  and the first powers of  $U_1$  cancel out. The remaining terms can be rearranged to yield

$$\left(\frac{\alpha}{2} - \beta\right)\xi^{-2\beta-1}W_1^2 + (\alpha - \chi)\xi^{-\chi-1}\kappa_1 - \frac{\alpha}{2}\xi^{-2\alpha-1}U_1^2 = 0. \quad (54)$$

Requiring

$$\beta = \alpha/2, \quad (55)$$

$$\chi = \alpha \quad (56)$$

allows the energy equation to be satisfied within an error of order  $\mathcal{O}(\xi^{-2\alpha-1})$ . This estimate will be refined in Sec. II C by using the information on the wall-normal velocities. The conditions (55) and (56) indicate that the contributions from transversal motion and turbulent kinetic energy to the total energy are comparable.

### C. Growth and entrainment rate

We now consider the growth rate of the jet in the span-wise and wall-normal directions. For the growth in the span-wise direction, we examine the span-wise displacement of the edge of the jet over a short distance  $d\xi$ ,

$$d\zeta = \frac{d\zeta}{d\xi}d\xi = \frac{d\zeta}{d\tau}\left(\frac{d\xi}{d\tau}\right)^{-1}d\zeta = \frac{w}{u}d\zeta, \quad (57)$$

hence,

$$\frac{d\zeta}{d\xi} \approx \frac{W_1^{-\alpha/2}}{\xi}. \quad (58)$$

Integrating along the streamwise direction, we obtain

$$\frac{a}{D} \approx \xi^{1-\alpha/2}, \quad (59)$$

$$\frac{b}{D} \approx \xi^{3\alpha/2-1}. \quad (60)$$

Equation (60) allows an estimate to be made for the magnitude of the wall-normal velocities within the jet. Differentiating with respect to  $\xi$  and reversing the chain of arguments leading to Eq. (58), one finds

$$V \approx \xi^{3\alpha/2-2}. \quad (61)$$

Equation (61) confirms the validity of the initial approximation made by neglecting the contribution of the vertical velocity component to

the kinetic energy. If the jet is identified as a rectangular area of size  $S$ , the mass flow rate carried by jet is

$$\frac{\mathcal{F}}{\rho_e U_e D^2} = \phi = \sigma \rho U = \sigma_1 \xi^\alpha + \mathcal{O}(\xi^{2\alpha}). \quad (62)$$

The entrainment rate is, therefore,

$$\rho U_e D \frac{d\phi}{d\xi} = \alpha \sigma_1 \xi^{\alpha-1} + \mathcal{O}(\xi^{2\alpha-1}). \quad (63)$$

## III. RESULTS

### A. Flow configuration

The theory developed in Sec. II is now tested on a set of numerical results. The results represent a family of well-documented film-cooling experiments. The experiments have been described in detail by Wittig *et al.*<sup>38</sup> The experiments represent single film cooling holes of cylindrical and fan-shaped cross section with an axis forming an angle of  $30^\circ$  to the direction of the wall. The ratio of hole length to diameter is  $L/D = 6$ . The holes discharge into the main channel where a fully developed turbulent flow of hot gas is established. The Mach number in the main channel is  $M_e = 0.6$ , and the boundary layer thickness upstream of the injection location is  $\delta/D = 0.5$ . The experiments are conducted with blowing ratios  $M = 0.5$ ,  $M = 1.0$ , and  $M = 1.5$ . Further details about the experimental setup are reported in Thole *et al.*<sup>2</sup> and Gritsch *et al.*<sup>39</sup>

### B. Numerical setup

The computations are based on a density-based code. The code is formally third-order accurate in time and space and adopts an implicit LES approach. The space discretization is cell-centered and uses MUSCL variable extrapolation to achieve spatial accuracy. Inviscid numerical fluxes are evaluated using Roe's Riemann solver. Inflow boundary conditions are imposed using a procedure developed by the authors<sup>40</sup> and reproducing realistic estimates of the two-point correlation tensor of the incoming turbulent flow. Full details of the numerical procedure, together with validation data based on the set of experiments by Wittig *et al.*,<sup>38</sup> are found in Hao and di Mare.<sup>41</sup> For the purpose of the present calculations, a computational domain comprising the main channel, the hole, and its plenum is formed and discretized with multiblock grids. The grids are created starting with the plenum and the main channel. Stubs of the cooling film are added to the two domains, and the two stubs are joined at the common surface. The block layouts for the stubs are selected from templates according to the geometry of the film and its insertion angle. All grids are initially created using very coarse resolution. The grids used for the computations are obtained from these initial grids by successive rounds of refinement and smoothing with attraction toward the walls to guarantee sufficient near-wall resolution. The complete procedure is described by Hao *et al.*,<sup>42</sup> Hao,<sup>43</sup> and Hao *et al.*<sup>44</sup> The domain extends 10D upstream of the injection location and 30D downstream. At the start of each computation, the LES simulation is run for around five flow-through times to eliminate the initial transient effects. Following that, statistics are collected for at least ten flow-through times for each case. The Courant number is 0.8.



### C. Downstream evolution of velocity defect and thickness

The downstream evolution of the velocity defect  $\Delta U$  for the two types of films is shown in Fig. 4. The exponent  $\alpha$  is determined via least squares fit for the far-field of the two types of jet, and it is found to be  $\alpha = -5/6$  for the fan-shaped film and  $\alpha = -13/15$  for the cylindrical film. The values obtained from the analysis of the velocity defect data are, then, used to obtain the exponent of the power law for the jet layer thickness  $b/D$  using Eq. (60). The power laws, thus, obtained are compared with the variation of  $b/D$  obtained directly from the computations. In both cases, the agreement between the observed power law and the predicted power law based on the velocity defect data is excellent.

### D. Mean flow quantities

The mean flow profiles are shown for fan-shape and cylindrical films in Fig. 5.  $\eta$  is the normalized distance from the wall. The profiles are extracted at distances between 5 and 20 orifice diameters downstream of the injection point and scaled according to the proposed scaling laws. The colored bands around the lines indicate the scatter of data taken on the jet centerline in the interval of  $5 < \xi < 20$ . Narrow areas indicated the collapse of the data onto a single master curve, which represents a universal self-similar profile. The mean velocity defect profiles for the fan-shaped film show uniformly good collapse of all data between  $x/D = 5$  and  $x/D = 20$ , regardless of the blowing ratio. This finding is consistent with historical evidence on the collapse of wall jet and wall wake velocity profiles both in two and three dimensions. Similarly, good collapse can be obtained for the cylindrical film data, with the exception that it is now not possible to overlay data from different blowing ratios on a single curve. The data for wall-normal velocity in fan-shaped films corroborate the assumption in Eq. (28) that the normal velocity is small and, therefore, its contribution to the kinetic energy of the jet is small. It is also clear that the wall-normal velocity in the wall jet formed by a fan-shaped film is negative: This is a mere consequence of continuity and of the relatively high lateral spreading rate of the jet. In essence, the jet moves fluid from its

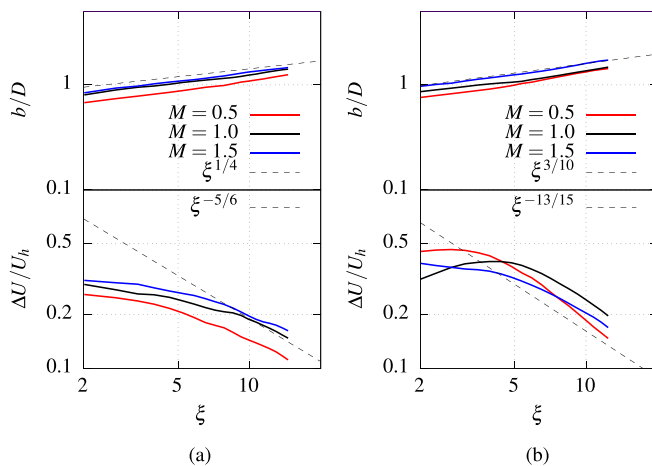


FIG. 4. Downstream evolution of velocity defect and jet layer thickness. (a) Fan-shaped film and (b) cylindrical film.

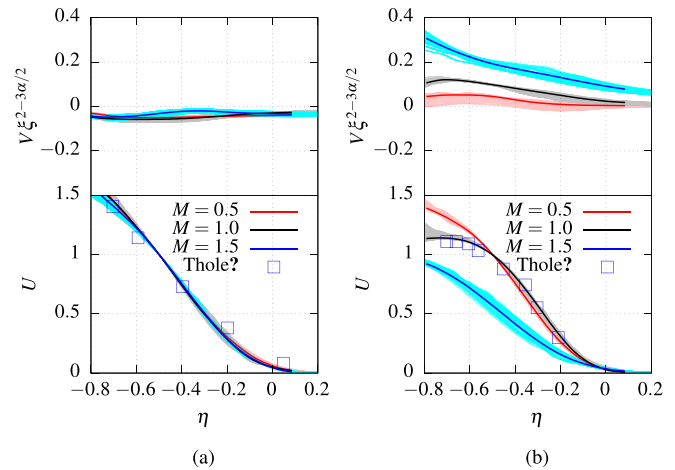


FIG. 5. Mean velocity defect and wall normal velocities. The colored bands around the lines indicate the scatter of data taken on the jet centerline in the interval of  $5 < \xi < 20$ . (a) Fan-shaped film and (b) cylindrical film.

upper side toward the wall and outwards toward its left and right edges. The collapse of wall-normal velocity data for the fan-shaped film in Fig. 5 also shows that the exponent  $2 - 3\alpha/2$  for the scaling of the vertical velocity is correct. The kinematics of the cylindrical jet is qualitatively different. Here, the fluid is drawn upwards, away from the wall, whereas the footprint of the jet on the wall grows narrower as the jet evolves downstream.

In Fig. 5, data from the experiment reported in Thole *et al.*<sup>2</sup> are also analyzed based on the proposed scaling law and plotted for both the fan-shaped film and the cylindrical film. The experiment data are shown to collapse well with the simulated data. This additional data source can justify the proposed scaling law.

### E. Reynolds stress

The Reynolds stress profiles are shown for fan-shape and cylindrical films in Fig. 6. The data in Fig. 6 need to be seen in the context of data for Reynolds stress in wall jets. The evidence so far on wall jets shows that the Reynolds stress data do not result in self-similar profiles when normalized with  $U_m^2$ . No systematic study exists of the self-similar properties of Reynolds stress profiles in film-cooling wall jets. Equation (56) shows that the Reynolds stress field in the wall jet of a film cooling device does not scale with the velocity defect squared. More precisely, Eq. (56) shows that when the Reynolds stresses or turbulence intensities are normalized by the velocity defect squared, the quantity intensifies scales like  $\xi^{-\alpha}$ . Some authors in the past have circumvented this difficulty by reporting Reynolds stresses normalized by the maximum value of the turbulent kinetic energy. The data in Fig. 6 show that by introducing the additional dependency on  $\xi$  predicted by the proposed theory, the collapse of Reynolds stress data can be still obtained for fan-shaped films. The exponent  $\beta = \alpha$  is shown to be the correct exponent to rescale turbulence intensity and Reynolds stress. The data reported in Fig. 6 also show that for fan-shaped films the magnitude of the Reynolds stress field can be scaled with the blowing ratio.

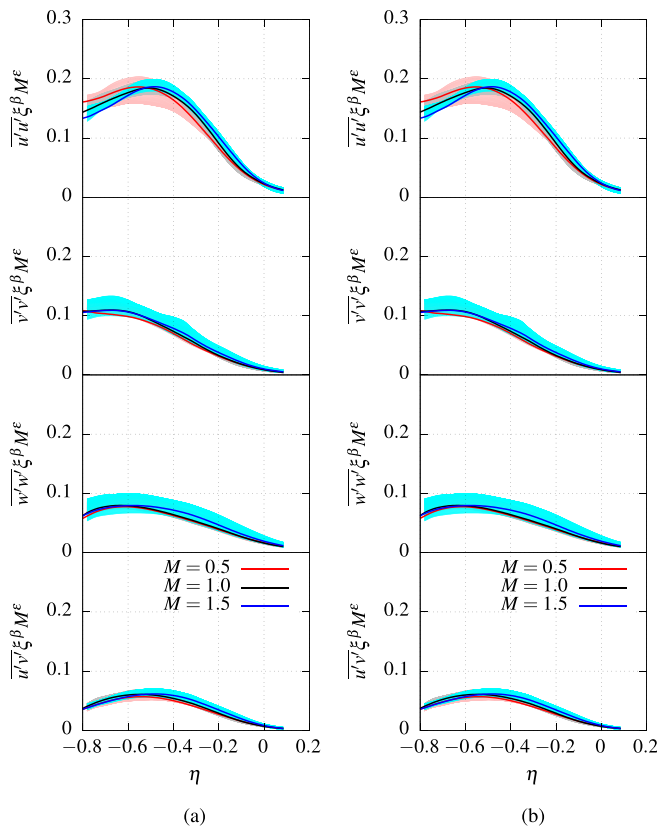


**FIG. 6.** Reynolds stresses. The colored bands around the lines indicate the scatter of data taken on the jet centerline in the interval  $5 < \xi < 20$ . (a) Fan-shape film and (b) cylindrical film.

The situation for cylindrical films, shown in Fig. 6, is slightly more complicated. In this case, no simple power law with respect to the blowing ratio  $M$  is suitable to rescale the Reynolds stress profiles. This happens because the different flow regimes—attached or lifted jets—represented in the current data impart different shapes to the Reynolds stress profile. Once the impossibility of collapsing curves from different blowing ratios is acknowledged, it is still possible to collapse data for each value of  $M$  separately. This is possible because the proposed theory can be applied to each flow condition separately. It is remarkable that, whereas different flow regimes result in different shapes of the Reynolds stress profiles, even for cylindrical films the algebraic relations binding the exponents  $\alpha$  and  $\beta$  still hold and the values of this exponent are shown to be fairly insensitive to the blowing ratio.

#### IV. CONCLUSIONS

Historical data on the wall jet show a clear consensus on the universality of mean velocity profiles and the downstream variation of the scaling parameters  $U_m$  and  $y_{m/2}$ . No such consensus exists on the scaling of the turbulent quantities. The authors derive a set of scaling laws for the mean and turbulent flow quantities from prime principles. The first step in the derivation is to idealize the area occupied by the jet as a rectangular area. Mass, momentum, and energy fluxes are written in terms of uniform free-stream quantities and mean quantities within the

jet. A set of relations is obtained describing the streamwise variation of streamwise velocity defect, density perturbation, span-wise and normal velocity, and turbulence intensity. It is shown that not all these quantities decay with the laws of the same power, but all can be expressed in terms of the exponent  $\alpha$  describing the decay of the velocity defect evaluated at a suitably chosen point along the jet layer thickness. One of the consequences of the scaling laws identified is that the correct scale for the turbulence intensity cannot be the velocity deficit squared. Furthermore, the shear stress at the wall is shown to be at most of the order  $-2\alpha$ . It is also shown that the large difference between span-wise and wall-normal growth rates observed in wall jets is a consequence of the conservation of momentum and energy, and of the initial hypothesis that the wall-normal velocities must be small. Numerical data indicate that the proposed theory is an accurate representation of the jet produced by a fan-shaped cooling film. It is also shown that for this type of device the wall-normal velocity profiles, velocity defects, and Reynolds stress profiles have shapes essentially independent of the blowing ratio  $M$ . A power law can also be identified that makes Reynolds stress data at various values of  $M$  collapse onto each other.

The jet produced by a cylindrical hole has a different flow arrangement. Nonetheless, power laws for the downstream development of velocity defect, transversal velocity scale, jet layer thickness, and turbulence intensity scale are derived in an identical fashion. The power laws obtained are shown to apply equally well to cylindrical films, albeit with modified exponents for the stream-wise decay of the velocity defect and growth of the jet layer thickness. It is seen that the velocity defect, wall-normal velocity, and Reynolds stress profiles have shapes sensitive to the blowing ratio  $M$ . As a consequence, it is not possible to identify a power law with respect to  $M$  that makes Reynolds stress profiles at various values of  $M$  collapse.

#### ACKNOWLEDGMENTS

Rolls-Royce plc is gratefully acknowledged for supporting this work and for granting permission for its publication. The research is under Grant No. DFR03150. The authors sincerely thank Romero Eduardo, Frederic Goenaga, Cristian Orozco Pineiro, and Haidong Li from Rolls-Royce plc for helpful discussions. The authors also acknowledge the use of the University of Oxford Advanced Research Computing367 (ARC), the facility in carrying out this work. <http://dx.doi.org/10.5281/zenodo.22558>. Part of this work was also performed using resources provided by the Cambridge Service for Data Driven Discovery (CSD3) operated by the University of Cambridge Research Computing Service ([www.csd3.cam.ac.uk](http://www.csd3.cam.ac.uk)), provided by Dell EMC and Intel using Tier-2 funding from the Engineering and Physical Sciences Research Council (Capital Grant No. EP/T022159/1) and DiRAC funding from the Science and Technology Facilities Council ([www.dirac.ac.uk](http://www.dirac.ac.uk)).

#### AUTHOR DECLARATIONS

##### Conflict of Interest

The authors have no conflicts to disclose.

#### Author Contributions

**Muting Hao:** Conceptualization (equal); Data curation (equal); Formal analysis (equal); Investigation (equal); Methodology (equal);

Software (equal); Visualization (equal); Writing – original draft (equal); Writing – review & editing (equal). **Luca di Mare:** Conceptualization (equal); Data curation (equal); Funding acquisition (equal); Methodology (equal); Project administration (equal); Supervision (equal); Writing – original draft (equal); Writing – review & editing (equal).

## DATA AVAILABILITY

The data that support the findings of this study are available from the corresponding author upon reasonable request.

## REFERENCES

- <sup>1</sup>B. Launder and W. Rodi, "The turbulent wall jet," *Prog. Aerosp. Sci.* **19**, 81–128 (1979).
- <sup>2</sup>K. Thole, M. Gritsch, A. Schulz, and S. Wittig, "Flowfield measurements for film-cooling holes with expanded exits," in *Heat Transfer Electric Power Industrial and Cogeneration* (American Society of Mechanical Engineers, 1996), Vol. 4.
- <sup>3</sup>G. J. Sturgess, "Wall cooling by gaseous injection for a high-performance combustion system," Ph.D. thesis (Loughborough University, 1971).
- <sup>4</sup>D. Singelmann and H. Mueller, "BMW rocket-engine development," Technical Report No. F-TR-2201-ND (Air Materiel Command Wright-Patterson, AFB, OH, 1948).
- <sup>5</sup>E. Förthmann, "Turbulent Jet Expansion," Report No. NACA TM-789, 1936.
- <sup>6</sup>H. W. Liepmann and J. Laufer, "Investigations of free turbulent mixing," Technical Report No. TN-1257 (NACA, 1947).
- <sup>7</sup>M. B. Glauert, "The wall jet," *J. Fluid Mech.* **1**, 625–643 (1956).
- <sup>8</sup>P. Bakke, "An experimental investigation of a wall jet," *J. Fluid Mech.* **2**, 467–472 (1957).
- <sup>9</sup>A. Sigalla, "Measurements of skin friction in a plane turbulent wall jet," *J. R. Aeronaut. Soc.* **62**, 873–877 (1958).
- <sup>10</sup>A. Sigalla, "Experimental data on turbulent wall jets: A correlation of existing data," *Aircr. Eng. Aerosp. Technol.* **30**, 131 (1958).
- <sup>11</sup>W. H. Schwarz and W. P. Cosart, "The two-dimensional turbulent wall-jet," *J. Fluid Mech.* **10**, 481–495 (1961).
- <sup>12</sup>A. Verhoff, *The Two-Dimensional, Turbulent Wall Jet With and Without an External Free Stream* (Princeton University, 1963).
- <sup>13</sup>V. Kruka and S. Eskinazi, "The wall-jet in a moving stream," *J. Fluid Mech.* **20**, 555–579 (1964).
- <sup>14</sup>M. Poreh, Y. G. Tsuei, and J. E. Cermak, "Investigation of a turbulent radial wall jet," *J. Appl. Mech.* **34**, 457–463 (1967).
- <sup>15</sup>P. Bradshaw and M. Gee, "Turbulent wall jets with and without an external stream," Ministry of Aviation Aeronautical Research Council Report and Memoranda No. 3252, 1960.
- <sup>16</sup>S. C. Kacker and J. H. Whitelaw, "Some properties of the two-dimensional, turbulent wall jet in a moving stream," *J. Appl. Mech.* **35**, 641–651 (1968).
- <sup>17</sup>S. C. Kacker and J. H. Whitelaw, "The turbulence characteristics of two-dimensional wall-jet and wall-wake flows," *J. Appl. Mech.* **38**, 239–252 (1971).
- <sup>18</sup>In cooling flows, effectiveness is a non-dimensional enthalpy used to quantify the ability of the cooling flow to shield the cooled wall from the hot free-stream.
- <sup>19</sup>G. J. Sturgess, "Account of film turbulence for predicting film cooling effectiveness in gas turbine combustors," *J. Eng. Power* **102**, 524–534 (1980).
- <sup>20</sup>G. J. Sturgess, "Design of combustor cooling slots for high film effectiveness: Part I—Film general development," *J. Eng. Gas Turbines Power* **108**, 354–360 (1986).
- <sup>21</sup>G. J. Sturgess and G. D. Pfeifer, "Design of combustor cooling slots for high film effectiveness: Part II—Film initial region," *J. Eng. Gas Turbines Power* **108**, 361–369 (1986).
- <sup>22</sup>G. P. Hammond, "Complete velocity profile and 'optimum' skin friction formulas for the plane wall-jet," *J. Fluids Eng.* **104**, 59–65 (1982).
- <sup>23</sup>D. B. Spalding, "A single formula for the 'Law of the wall,'" *J. Appl. Mech.* **28**, 455–458 (1961).
- <sup>24</sup>D. Coles, "The law of the wake in the turbulent boundary layer," *J. Fluid Mech.* **1**, 191–226 (1956).
- <sup>25</sup>B. Launder and W. Rodi, "The turbulent wall jet measurements and modeling," *Annu. Rev. Fluid Mech.* **15**, 429–459 (1983).
- <sup>26</sup>I. Wygnanski, Y. Katz, and E. Horev, "On the applicability of various scaling laws to the turbulent wall jet," *J. Fluid Mech.* **234**, 669–690 (1992).
- <sup>27</sup>M. Zhou and I. Wygnanski, "Parameters governing the turbulent wall jet in an external stream," *AIAA J.* **31**, 848–853 (1993).
- <sup>28</sup>J. G. Eriksson, R. I. Karlsson, and J. Persson, "An experimental study of a two-dimensional plane turbulent wall jet," *Exp. Fluids* **25**, 50–60 (1998).
- <sup>29</sup>W. K. George, H. Abrahamsson, J. Eriksson, R. I. Karlsson, L. Löfdahl, and M. Wosnik, "A similarity theory for the turbulent plane wall jet without external stream," *J. Fluid Mech.* **425**, 367–411 (2000).
- <sup>30</sup>G. I. Barenblatt, A. J. Chorin, and V. M. Prostokishin, "The turbulent wall jet: A triple-layered structure and incomplete similarity," *Proc. Natl. Acad. Sci.* **102**, 8850–8853 (2005).
- <sup>31</sup>A. Gupta, H. Choudhary, A. K. Singh, T. Prabhakaran, and S. A. Dixit, "Scaling mean velocity in two-dimensional turbulent wall jets," *J. Fluid Mech.* **891**, A11 (2020).
- <sup>32</sup>P. M. Sforza and G. Herbst, "A study of three-dimensional, incompressible, turbulent wall jets," *AIAA J.* **8**, 276–283 (1970).
- <sup>33</sup>A. T. Kirkpatrick and A. E. Kenyon, "Flow characteristics of three-dimensional wall jets," *Trans. Am. Soc. Heat, Refrig. Air Cond. Eng.* **104**, 1755–1762 (1998), see <https://www.aivc.org/resource/flow-characteristics-three-dimensional-wall-jets>.
- <sup>34</sup>B. G. Newman, R. P. Patel, S. B. Savage, and H. K. Tjio, "Three-dimensional wall jet originating from a circular orifice," *Aeronaut. Q.* **23**, 188–200 (1972).
- <sup>35</sup>N. V. C. Swamy and P. Bandyopadhyay, "Mean and turbulence characteristics of three-dimensional wall jets," *J. Fluid Mech.* **71**, 541–562 (1975).
- <sup>36</sup>L. Namgyal and J. W. Hall, "Reynolds stress distribution and turbulence generated secondary flow in the turbulent three-dimensional wall jet," *J. Fluid Mech.* **800**, 613–644 (2016).
- <sup>37</sup>T. J. Craft and B. E. Launder, "On the spreading mechanism of the three-dimensional turbulent wall jet," *J. Fluid Mech.* **435**, 305–326 (2001).
- <sup>38</sup>S. Wittig, A. Schulz, M. Gritsch, and K. A. Thole, "Transonic film-cooling investigations: Effects of hole shapes and orientations," in *Turbo Expo: Power for Land, Sea, and Air* (American Society of Mechanical Engineers, 1996).
- <sup>39</sup>M. Gritsch, A. Schulz, and S. Wittig, "Adiabatic wall effectiveness measurements of film-cooling holes with expanded exits," in *Heat Transfer Electric Power Industrial and Cogeneration* (American Society of Mechanical Engineers, 1997), Vol. 3.
- <sup>40</sup>M. Hao, J. Hope-Collins, and L. di Mare, "Generation of turbulent inflow data from realistic approximations of the covariance tensor," *Phys. Fluids* **34**, 115140 (2022).
- <sup>41</sup>M. Hao and L. di Mare, "Reynolds stresses and turbulent heat fluxes in fan-shaped and cylindrical film cooling holes," *Int. J. Heat Mass Transfer* **214**, 124324 (2023).
- <sup>42</sup>M. Hao, F. Wang, J. Hope-Collins, M. E. Rife, and L. di Mare, "Template-based hexahedral mesh generation for turbine cooling geometries," in *Turbo Expo: Power for Land, Sea, and Air* (American Society of Mechanical Engineers, 2020).
- <sup>43</sup>M. Hao, "Numerical methods for unsteady film cooling in gas turbine," Ph.D. thesis (The University of Oxford, 2023).
- <sup>44</sup>M. Hao and L. di Mare, "Budgets of Reynolds stresses in film cooling with fan-shaped and cylindrical holes," *Phys. Fluids* (in press) (2023).